Separation Science and Technology

Publication details, including instructions for authors and subscription information:
http://www.informaworld.com/smpp/title~content=t713708471

Modeling of Adsorptive Filtration of a Leather Dye in a Fixed Bed Column

Ticiane P. Sauer[a]; Leonardo Casaril[a]; André L. B. Oberziner[a]; José L. Soares[a]; Regina de F. P. M. Moreira[a]
[a] Department of Chemical and Food Engineering, Federal University of Santa Catarina, Florianópolis, Santa Catarina, Brazil

To cite this Article Sauer, Ticiane P. , Casaril, Leonardo , Oberziner, André L. B. , Soares, José L. and Moreira, Regina de F. P. M.(2006) 'Modeling of Adsorptive Filtration of a Leather Dye in a Fixed Bed Column', Separation Science and Technology, 41: 3, 501 — 513

To link to this Article: DOI: 10.1080/01496390500460765

URL: http://dx.doi.org/10.1080/01496390500460765

Separation Science and Technology, 41: 501–513, 2006

ISSN 0149-6395 print/1520-5754 online
DOI: 10.1080/01496390500460765

Modeling of Adsorptive Filtration of a Leather Dye in a Fixed Bed Column

Ticiane P. Sauer, Leonardo Casaril, André L. B. Oberziner,
José L. Soares, and Regina de F. P. M. Moreira
Department of Chemical and Food Engineering,
Federal University of Santa Catarina, Florianópolis, Santa Catarina, Brazil

Abstract: Activated carbons offer an efficient option for the removal of organic and inorganic contaminants from water. However, due to its high costs and difficulty in the regeneration, other low cost adsorbents have been used. In this work, the adsorption capacity of an adsorbent carbon with high iron oxides concentration was compared with that of a commercial activated carbon in the removal of a leather dye from an aqueous solution. The adsorbents were characterized using SEM/EDAX analysis and BET surface area. The capacity of adsorption of the adsorbents was evaluated through the static method at 25°C. The results showed that the color removal was due to the adsorption and precipitation of the dye on the surface of the solids. The adsorption equilibrium was described according to the linear model for the adsorbent carbon and the equilibrium constant was $0.02\,\mathrm{L\,g^{-1}}$. The equilibrium of adsorption on activated carbon exhibited a behavior typical of the Langmuir isotherm and the monolayer coverage was $24.33\,\mathrm{mg\,g^{-1}}$. A mathematical model was proposed to describe the dynamics of the color removal using a fixed bed considering that the color removal is due to the adsorption and the precipitation of the dye on the adsorbent.

Keywords: Adsorption, color removal, modeling, water treatment

INTRODUCTION

Present environmental legislation is very rigorous in almost all leather producing countries. Consequently, wastewater treatment is a matter of

Received 12 September 2005, Accepted 6 November 2005

Address correspondence to Regina de F. P. M. Moreira, Department of Chemical and Food Engineering, Federal University of Santa Catarina, Campus Universitário, Trindade, 88040-900, Florianópolis, Santa Catarina, Brazil. E-mail: regina@enq.ufsc.br

some urgency in most tanneries. The traditional method of purification of tannery wastewater was to mix all the effluents produced in several parts of the tanning process and treat it by physico-chemical and biological processes. Nowadays, it is more common to treat the wastewater produced in each part of the process separately. This scheme provides good results and has been adopted by a number of tanneries throughout the world (1). However, some improvements can be made to reduce the color of effluents, mainly those from dyeing processes, in order to achieve the limit concentration of $75\,\mathrm{mg \cdot L^{-1}}$ PtCo to final discharge, according to Brazilian regulation (2).

Activated carbon can be used as an adsorbent to remove several organic compounds, but its high cost frequently prevents its use in tannery industries. Clays such as bentonite and sepiolite were recently reported as useful adsorbents for the removal of surfactants and dyes (1), but generally they are available only as small particles rendering their use in fixed bed columns unpracticable.

Numerous studies (3–5) have demonstrated that Fe/Mn/Al hydrous oxides and organic surface coatings substantially influence the sorptive behavior of a solid. Novel adsorbents produced by controlled deposition of iron oxides on a porous support have recently been reported (5–7). These iron oxide-coated media have been used as alternatives to activated carbon in the removal of metals and organic compounds (3, 6–9).

The adsorptive capacity of iron oxide-coated media results from the relatively high surface area and surface charge of iron oxides (3). The support of the iron oxide-coated media should have special properties to allow high adherence and stability of the media to permit its use for several adsorption/regeneration cycles (10).

The dye adsorption on single sorbents has been studied extensively, but the adsorption with hybrid sorbents requires further investigation. In this work we investigated the removal of a leather dye in aqueous solution by adsorption using an adsorbent carbon with high iron oxides concentration and activated carbon in a fixed bed column.

DYNAMICS OF ADSORPTIVE FILTRATION IN A FIXED BED COLUMN

When the adsorption is the only mechanism for the solute removal, the total amount of solute adsorbed on the solid surface in a fixed bed column can be evaluated through mass balance according to Equation (1).

$$t_{st} = \frac{V}{Q}\left[\varepsilon + (1-\varepsilon)\rho_s \frac{q}{C_o}\right] = \int_0^{\infty}\left(1 - \frac{C}{C_0}\right)dt \qquad (1)$$

where t_{st} is the stoichiometric time, V is the bed volume, Q is the flow rate, ε is the bed porosity, ρ is the specific mass of the adsorbent, C_0 is the concentration of the solute at the inlet of the column and q is the amount of solute adsorbed on the solid surface in equilibrium with the amount of solute in the liquid phase.

It has been reported that the removal of heavy metals and some organic compounds in a fixed bed column using iron oxide-coated media is due to two simultaneous mechanisms, the surface adsorption and precipitation on iron oxide and support surfaces (4). Surface adsorption is generally a fast process that reaches equilibrium rapidly, and the precipitation and co-precipitation in solution or diffusion through the iron oxides and surface precipitation are much slower processes. The precipitation can be modeled as a first-order loss reaction (4).

The one-dimensional mass balance equation considering a first-order loss term that describes the leather dye removal is given by Equation (2).

$$\frac{1}{Pe}\frac{\partial^2 C_i}{\partial x^2} - \frac{\partial C_i}{\partial x} = \frac{\partial C_i}{\partial \theta} + \frac{\rho_L}{\varepsilon}\frac{\partial \bar{q}_i}{\partial \theta} + \tau k C_i = 0 \qquad (2)$$

where x is dimensionless axial coordinate ($x = z/L$), z is axial coordinate in the bed, L is the bed length; θ is the dimensionless time ($\theta = t/\tau$), t is the time, ρ_s is the solid density, ε is the bed porosity, k is the pseudo-first order constant, C_i is the molar concentration, $\bar{q}_i$ is the average adsorbed concentration and Pe is the Peclet number (Eq. 3) and τ is defined in Equation (4).

$$Pe = \frac{\nu \cdot L}{D} \qquad (3)$$

$$\tau = \frac{L}{\nu} \qquad (4)$$

where ν is interstitial velocity and D is the axial dispersion coefficient.

The term $\partial q_i/\partial t$ represents the global rate of mass transfer of the solute in the particle and can be described according to the linear driving force model (Eq. 5).

$$\frac{\partial \bar{q}_i}{\partial \theta} = k_s \tau (q_i^* - q_i) \qquad (5)$$

where k_s is the internal mass transfer coefficient and q^* adsorbed concentration at equilibrium.

The equilibrium of adsorption is described by thermodynamic models, such as a linear isotherm (Eq. 6) or the Langmuir model (Eq. 7).

$$q^* = k \cdot C \qquad (6)$$

$$q^* = \frac{q_m b C}{(1 + bC)} \qquad (7)$$

By introducing the boundary conditions (Eq. 8)

$$\begin{aligned} &\theta = 0: && \bar{q} = 0; && C = 0 \\ &x = 0: && -\frac{1}{Pe}\frac{\partial C}{\partial x} + C = C_0; && \\ &x = 1: && \frac{\partial C}{\partial x} = 0; && \end{aligned} \tag{8}$$

Equations 2 to 8 can be solved using a computational package PDECOL (11) using FORTRAN language, based on the orthogonal collocation method of finite elements for partial differential equations in double precision. In this work, we used 50 elements to simulate the experimental results, with 2 collocation points for each element and a tolerance of 10^{-9}.

The Peclet number (Pe) was evaluated according to Equation 9 (12).

$$Pe = \frac{0.508\,\mathrm{Re}^{0.02}\,L}{dP} \tag{9}$$

where Re is the Reynolds number (Eq. 10).

$$Re = \frac{\rho \cdot \nu \cdot dp}{\mu\,(1 - \varepsilon)} \tag{10}$$

The input parameters included porosity (ε), dry solids density of the sorbent (ρ), dye concentration at the inlet column (C_o) and velocity of the aqueous solution (ν).

MATERIAL AND METHODS

Material

The activated carbon (PK35) was supplied by Norit (The Netherlands). The adsorbent carbon with high iron oxides concentration was supplied by Carbonífera Criciúma S.A. (Brazil).

Direct Black 38, a dye extensively used in the leather industry, was used as a model compound. Table 1 shows some properties and the chemical structure of this compound, and the wavelength at which maximum absorption of light occurs, λ_{max}.

Sorption Equilibrium

A series of fixed volumes (200 mL) of solutions with predetermined initial dye concentrations were prepared and brought into contact with predetermined masses (1 g) of adsorbent. The flasks were sealed and shaken in a shaker (60 rev min^{-1} shaking rate) at constant temperature $25 \pm 1°\mathrm{C}$ for 24 hours until equilibrium was reached. The pH was adjusted to 2.5 using H_2SO_4

Table 1. Information regarding the Direct Black 38 dye

Name	Direct Black 38
CAS Number	1937-37-7
Molecular weight, g mol^{-1}	781.73
Water solubility at 20°C, g L^{-1}	1–5
λ_{max} (nm)	590
Molecular formula	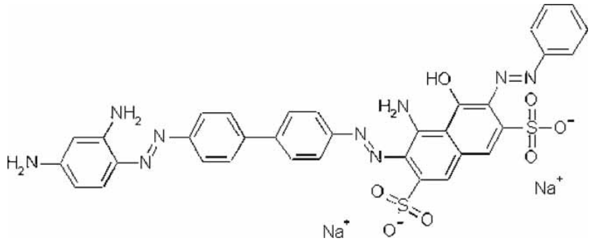

solution and was maintained constant during the adsorption. The concentration of dye remaining in the aqueous solution was determined by UV-vis spectrophotometry at $\lambda_{max} = 590\,nm$, using a UV/vis spectrophotometer (Shimadzu UV1650C). The amount of the adsorbed dye on the solid surface was determined by mass balance.

Adsorption of Dye in a Fixed Bed Column

The column tests were performed in a column with 3 cm diameter column and 15 cm height. The column was filled with adsorbent. The solution was pumped to the column using a peristaltic pump (Masterflex) at a flow rate of 20 mL min^{-1}. The concentration of the dye at the end of the column was continuously monitored using a flow cell in a UV/vis spectrophotometer (Fig. 1). The inlet concentration was in the range 25–300 mg L^{-1}, at pH 2.5.

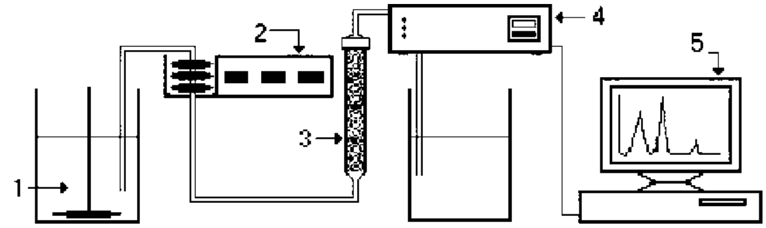

Figure 1. Scheme of the experimental system. (1-Aqueous solution reservoir, 2–Peristaltic pump, 3–Column, 4–UVvis Spectrophotometer, 5–Computer)

Characterization of the Adsorbents

Samples for SEM/EDAX (SEM/EDAX Philips XL-30, Scanning Electronic Microscope) analysis were coated with thin carbon film in order to avoid the influence of charge effect during the SEM operation in the analysis of the adsorbent carbon. Elemental microprobe and elemental distribution mapping techniques were used for analyzing the elemental distribution of solid samples. The scanning energy for EDAX analysis was from 0 to 10.23 KeV with an elapsed time of 100 s.

The BET surface area was determined by the nitrogen adsorption isotherm technique, with an Autosorb 1C (Quantachrome, USA) analyzer. The nitrogen adsorption was carried out at 77 K.

Mass titration proposed by Noh and Schwarz (1990) (13), which is an alternative method to the conventional acid–base titration technique, was carried out to estimate the point of zero charge (PZC) of the solids.

RESULTS AND DISCUSSION

Characterization of the Adsorbents

The SEM photographs in Fig. 2 were taken at 5000X and 1000X magnifications to observe the surface morphology of the adsorbent carbon and activated carbon, respectively. The adsorbent carbon had a rough surface and the presence of iron oxide aggregates uniformly coated the surface. The morphology of the activated carbon is typical for high porous materials. Table 2 shows the elemental composition obtained from the EDAX analysis.

Surface area for samples was investigated using BET analysis. The isotherm for N_2 adsorption at 77 K (Fig. 3) for the adsorbent carbon is typical for low porosity solids and presented a little hysteresis, indicating the presence of few mesopores.

The activated carbon presented a type IV isotherm (14), typical for solids with high amounts of micropores. The form of hysteresis may be related to the dominant pore shape in the mesoporous solid and the type shown by activated carbon is that found for slit-shaped pores, as is often seen for mesopores in activated carbons. The onset of the hysteresis loop in each isotherm took place at a relative pressure of approximately 0.4, which indicates that the action of the capillary condensation could have started from a pore size around 30 Å (15). The parameters for the textural and chemical characterization are summarized in Table 2.

Adsorption Equilibrium

The adsorption equilibriums for the dye adsorption on the two adsorbents had different behaviors, as shown in Fig. 4. The adsorption capacity of

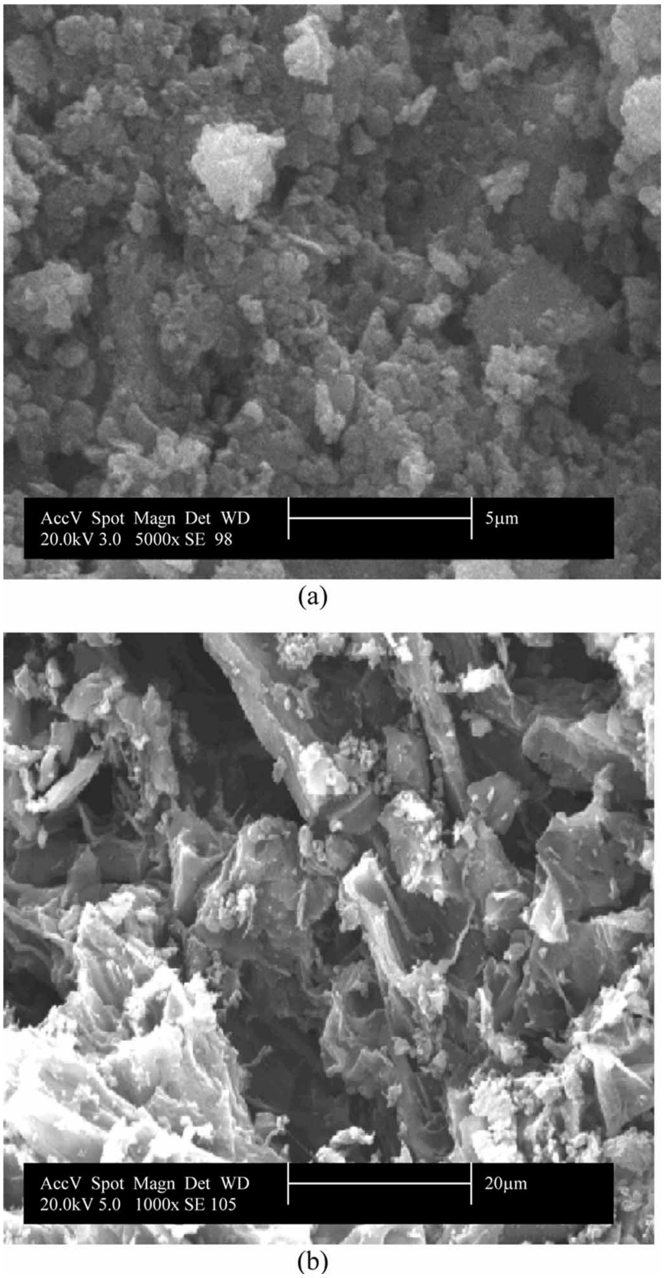

Figure 2. SEM micrographs of samples: (a) Adsorbent carbon; (b) Activated carbon.

Table 2. Chemical and textural characterization of the adsorbents

	Adsorbent carbon	Activated carbon
Point of zero charge	8.4	9.1
Proximate analysis, %		
Fixed carbon	28.75	81.9
Volatile	19.98	11.1
Ash	51.27	7.0
BET area, $m^2 g^{-1}$	5	659
Micropore volume, $cm^3 g^{-1}$	1.42×10^{-3}	0.309
Elemental analysis, % (w/w)		
C	31.25	68.86
O	17.89	27.88
Fe	21.04	nd*
Na	4.81	nd*
Al	8.25	0.40
Si	7.41	0.94
S	4.89	nd*
Ca	1.44	0.88
Mg	nd*	1.04
K	0.93	nd*
Ti	0.54	nd*
Cl	1.53	nd*

nd = not detected.

activated carbon is much higher than that of the adsorbent carbon, due to the high surface area of the activated carbon. The shape of the equilibrium isotherm of the dye on activated carbon is of a Langmuir type. The experimental data were well fitted to the Langmuir model (Eq. 7), resulting in a monolayer coverage of $24.33\,mg\,g^{-1}$. The adsorption of dye on the adsorbent carbon showed a linear isotherm, within the experimental error, and the equilibrium constant was $0.02\,L\,g^{-1}$.

Breakthrough Curves

The concentration of dye at the end of the column was continuously monitored, as described in the experimental section. However, even after very prolonged tests, the concentration of the dye at the end of the column did not achieve the value at the inlet, indicating that another simultaneous process had occurred (Figs. 5 and 6).

According Nikolaidis et al. (2003) (4), iron oxide-coated media removes solute dissolved in water by two simultaneous mechanisms, the surface adsorption and precipitation. Then, we developed a model previously described to simulate the experimental data.

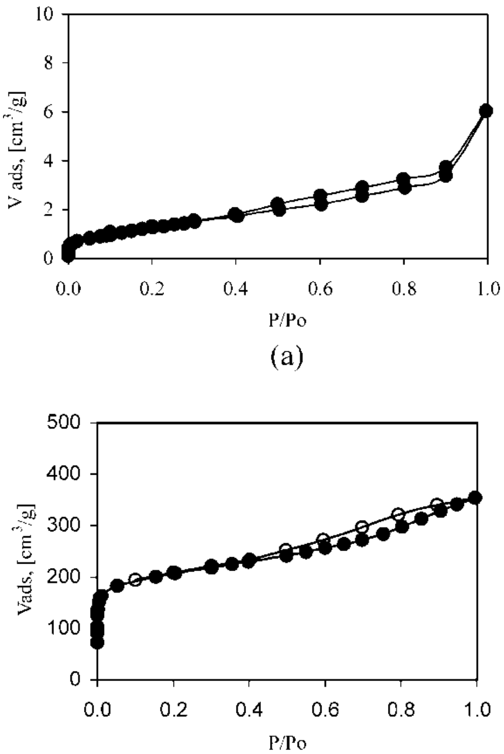

(a)

(b)

Figure 3. N_2 adsorption and desorption curves for the adsorbent carbon (a) and activated carbon (b).

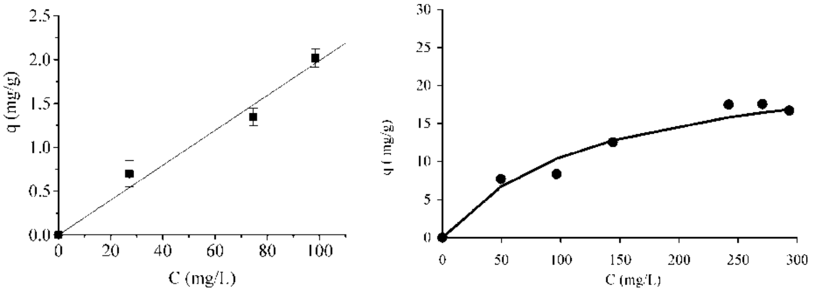

(a) (b)

Figure 4. Isotherm of dye adsorption on the adsorbent carbon (a) and activated carbon (b).

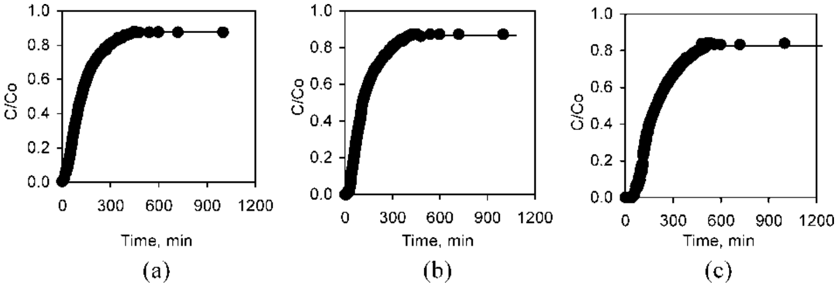

Figure 5. Breakthrough curves for the removal of dye on the composite, using different feed concentration of dye: (a) 49.8 mg L^{-1}, (b) 74.7 mg L^{-1}; (c) 98.4 mg L^{-1} (Symbols: experimental data; Line: simulated results).

Figures 5 and 6 show the experimental data and the simulated breakthrough curves for the removal of the dye on the adsorbent carbon and activated carbon. In the UV/vis spectrophotometric analysis of the dye no spectral changes were observable and we thus disregarded the possibility of chemical reactions. Desorption experiments were performed using distilled water as eluant in order to evaluate the amount of dye recovered by desorption and backwashing. The mass balance applied to the desorption data showed that the dye could be recovered by backwashing of the saturated adsorbent.

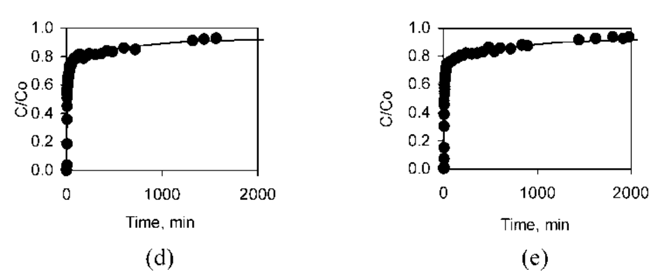

Figure 6. Breakthrough curves for the removal of dye on activated carbon, using different feed concentration of dye: (a) 75 mg L^{-1}, (b) 96 mg L^{-1}; (c) 192.8 mg L^{-1}; (d) 242.1 mg L^{-1}; (e) 270.8 mg L^{-1} (Symbols: experimental data; Line: simulated results).

Table 3. Parameters used to simulate the breakthrough curves for the dye removal on the activated carbon and the adsorbent carbon

	Activated carbon[a]					Adsorbent carbon[b]		
C_o, ppm	96.0	144.0	192.8	242.1	270.8	49.8	74.7	98.4
t_{st}, min	343.49	345.42	124.46	242.96	257.13	86.8	122.7	98.4
Re	0.32	0.32	0.42	0.42	0.42	1.06	0.96	0.96
Pe	413.8	413.8	416.0	416.0	416.0	101.7	101.5	101.5
k_s, min.$^{-1}$	0.0020	0.0019	0.0015	0.0015	0.0015	0.035	0.035	0.035
k, min.$^{-1}$	0.02	0.02	0.02	0.02	0.02	0.04	0.04	0.04

[a] Particle size (d_p) = 1 mm, bed porosity (ε) = 0.56.

[b] Particle size (d_p) = 0.81 mm, bed porosity (ε) = 0.51.

The simulated breakthrough curves shown in Figs. 5 and 6 were obtained using the parameters summarized in Table 3 and by calibration of k_s and k parameters in order to fit the model (Eq. 2) over the breakthrough experiments. k_s is the mass transfer constant according to Eq. (5) and k is the first-order constant that describes the precipitation on the solids surface and was not dependent on the concentration of solute in the liquid phase.

The capacity of dye adsorption using activated carbon in a fixed bed column is much higher than that using the adsorbent carbon, as measured in a batch system (Fig. 4). However, the kinetic of adsorption of dye using activated carbon is slower than that using the adsorbent carbon due to the diffusion of the dye inside the particles of the highly porous activated carbon, while the adsorption of the dye on the adsorbent carbon is basically restricted to the external surface.

The first-order constant that describes the precipitation on the solids surface of the adsorbent carbon is higher than that for activated carbon, since the iron oxide–coated surface generally has a gelatinous characteristic (10) that allows efficient retention between the particles. This is an advantageous aspect of using adsorbent carbon with high iron oxide concentration, because the regeneration can be achieved by backwashing of the saturated adsorbent.

CONCLUSIONS

In this study, an adsorbent carbon with high iron oxide concentration was used to remove a dye from an aqueous solution. The performance of the adsorbent was compared to that of a commercial activated carbon.

Activated carbon showed a higher adsorption capacity than of the adsorbent carbon due to its higher surface area. The removal of the dye in a fixed bed column showed that two simultaneous processes occur. Besides adsorption, it was observed that the dye can be removed by precipitation on the solids and it is retained between the solid particles. A mathematical model was developed to simulate the removal process according to a mass transfer process and a first-loss order precipitation. Calibration of these parameters using the experimental data gave a mass transfer coefficient for the dye adsorption on activated carbon, which indicated a slow process, due to the fine pores of the adsorbent. The first-order constant for the precipitation on the adsorbent carbon was higher than that for activated carbon due to the gelatinous characteristics of the iron oxide coated-surface of the adsorbent carbon, that retains easily the precipitates between the particles.

ACKNOWLEDGMENTS

The authors are grateful to CNPq/FINEP/CTHidro and Carbonífera Criciúma S.A. for financial support.

REFERENCES

1. Espantaleón, A.G., Nieto, J.A., Fernández, M., and Marsal, A. (2003) Use of activated clays in the removal of dyes and surfactants form tannery wastewaters. *Appl. Clay Sci.*, 24: 105.
2. Conselho Nacional de Meio Ambinente–CONAMA, Ministério do Meio Ambiente Resolução 357, March 17, 2005.
3. Lai, C.H. and Chen, C.Y. (2001) Removal of metal ions and humic acid from water by iron-coated filter media. *Chemosphere*, 44: 1177.
4. Nikolaidis, N.P., Dobbs, G.M., and Lackovic, J.A. (2003) Arsenic removal by zero-valent iron: field, laboratory and modeling studies. *Wat. Res.*, 37: 1417.
5. Xu, Y. and Axe, L. (2005) Synthesis and characterization of iron-oxide coated silica and its effect on metal adsorption. *J. Colloid and Interf. Sci.*, 282: 11.
6. Moreira, R.F.P.M., Madeira, V.S., and José, H.J (Dec. 21, 2004) Compósito granular para a remoção de contaminantes em águas e processos para produção dos mesmos. Brazil. Patent PI0405916-6.
7. Oliveira, L.C.A., Rios, R.V.R.A., Fabris, J.D., et al (2002) Activated carbon/iron oxide magnetic composites for the adsorption of contaminants in water. *Carbon*, 40: 2177.
8. Katsoyiannis, I.A. and Zouboulis, A.I. (2002) Removal of arsenic from contaminated water sources by sorption onto iron-oxide-coated polymeric materials. *Wat. Res.*, 36: 5141.
9. Moreira, R.F.P.M., Madeira, V.S., José, H.J., and Humeres, E. (2004) Removal of iron from water using adsorbent carbon. *Sep. Sci. Technol.*, 39 (1): 267.
10. Lai, C.H., Lo, S.L., and Chiang, H.L. (2000) Adsorption/desorption properties of copper ions on the surface of iron-coated sand using BET and EDAX analyses. *Chemosphere*, 41: 1249.
11. Madsen, N.K. and Sincovec, R.F. (1979) *PDECOL: General collocation software for partial differential equations*. ACM Trans. Math. Software.
12. Leitão, A. and Rodrigues, A.E. (1999) Modeling and simulation of protein adsorption in permeable chromatographic packings: a double linear driving force model. *Biochem. Eng. J.*, 3: 131.
13. Noh, J.S. and Schwarz, J.A. (1990) Effect of HNO_3 treatment on the surface acidity of activated carbons. *Carbon*, 28: 675.
14. Ruthven, D. (1980) *Principles of Adsorption and Adsorption Processes*; John Wiley & Sons, New York.
15. Claudino, A., Soares, J.L., Moreira, R.F.P.M., and José, H.J. (2004) Adsorption equilibrium and breakthrough analysis for NO adsorption on activated carbons at low temperatures. *Carbon*, 42: 1483.